Genes & Diseases (2026) 13, 101888

Available online at www.sciencedirect.com

ScienceDirect

journal homepage: www.keaipublishing.com/en/journals/genes-diseases

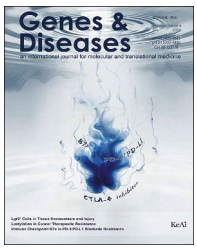

FULL LENGTH ARTICLE

# ATOX1 overexpression mitigates copper homeostasis in microglia: Implications for Alzheimer's disease therapy

**Fuxin Zhong [a,b,c,e], Jiani Wu [a,b,c,e], Zhangjing Deng [a,b,c,e], Wuhan Yu [a,b,c], Jiaqi Song [d], Yingxi Chen [d], Weihua Yu [d], Yang Lü [a,b,c,*]**

[a] *Department of Geriatrics, The First Affiliated Hospital of Chongqing Medical University, Chongqing 400016, China*
[b] *Key Laboratory of Major Brain Disease and Aging Research (Ministry of Education), Chongqing Medical University, Chongqing 400014, China*
[c] *Institute for Brain Science and Disease, Chongqing Medical University, Chongqing 400016, China*
[d] *Institute of Neuroscience, Department of Human Anatomy, Chongqing Medical University, Chongqing 400016, China*

Received 16 December 2024; received in revised form 6 July 2025; accepted 21 August 2025
Available online 18 October 2025

**KEYWORDS**
Alzheimer's disease;
ATOX1;
Copper;
Microglia;
Oxidative stress

**Abstract** Copper ($Cu^{2+}$) is a known contributor to the pathogenesis of Alzheimer's disease (AD). However, it is uncertain whether proteins regulating copper homeostasis affect $Cu^{2+}$ in microglia. Antioxidant protein 1 (ATOX1) plays a key role in $Cu^{2+}$ homeostasis, oxidative stress, and cell protection. Despite its critical functions, the role of ATOX1 in AD pathology remains poorly defined. This study aims to examine the effects of ATOX1 on oxidative stress, apoptosis, and neuroinflammation in microglia by modulating $Cu^{2+}$ homeostasis. *In vivo*, a 5 × FAD mouse model was used to investigate the localization and expression of ATOX1 in AD by immunofluorescence and three-dimensional reconstruction. The $A\beta_{1\text{-}42}$ oligomer was used to establish an AD model *in vitro*. The role of ATOX1 in $Cu^{2+}$ homeostasis regulation in microglia was further studied using co-immunoprecipitation, Western blotting, quantitative real-time PCR, and spectrophotometry. A reduction in ATOX1 expression was noted in Aβ-plaques-associated microglia compared with normal microglia. $Cu^{2+}$ levels were elevated in the *in vitro* AD model, and ATOX1 directly regulated copper homeostasis via P1B-ATPase (ATP7B) in microglia. Excessive $Cu^{2+}$ induced oxidative stress, neuroinflammation, and apoptosis. Overexpression of ATOX1 alleviated this neurotoxicity, indicating its potential to alleviate oxidative

* Corresponding author. Department of Geriatrics, The First Affiliated Hospital of Chongqing Medical University, No.1 Youyi Road, Yuzhong District, Chongqing 400016, China.
*E-mail address:* yanglyu@hospital.cqmu.edu.cn (Y. Lü).
Peer review under the responsibility of Chongqing Medical University.
[e] These authors contributed equally to this study.

https://doi.org/10.1016/j.gendis.2025.101888

stress, cell apoptosis, and neuroinflammation in AD. ATOX1 overexpression offers protective effects on microglia through $Cu^{2+}$ homeostasis, which may lead to potential therapeutic strategies for AD.


## Introduction

Alzheimer's disease (AD) is the most common form of dementia, characterized by a gradual decline in memory and cognitive functions.[1] The hallmark of AD pathology is the presence of β-amyloid (Aβ) plaques.[2] Numerous studies suggest that oxidative stress plays a key role in AD. Research has shown that copper ($Cu^{2+}$) can aggregate and generate reactive oxygen species (ROS) in the brain.[3] $Cu^{2+}$ interacts with Aβ, facilitating various redox reactions.[4] Recent studies have confirmed that the oxidative stress observed in AD is linked to the interaction between $Cu^{2+}$ and Aβ, leading to ROS production.[5] Moreover, several studies have indicated an increase in $Cu^{2+}$ concentration near Aβ-plaques in both AD patients and mouse models.[6–8] However, the precise mechanism of copper accumulation at the amyloid site remains unclear.

Heavy metals are stressors that induce the accumulation of ROS, apoptosis, and neuroinflammation.[9,10] Numerous studies have shown that prolonged exposure to $Cu^{2+}$ leads to ROS accumulation, resulting in mitochondrial dysfunction and apoptosis.[11–13] Apoptosis serves as an intracellular defense mechanism, and the changes in $Cu^{2+}$ levels can affect apoptosis signal transduction.[14] Previous research highlighted the role of anti-apoptotic factors, such as the B-cell lymphoma 2 (Bcl2) family, in regulating the response of microglia to Aβ-plaques.[15,16] Dysregulated $Cu^{2+}$ levels can disrupt the inflammatory balance, as evidenced by the $Cu^{2+}$ accumulation in microglia near Aβ-plaques and the resulting neurotoxic effects.[4] Some studies suggest that chronic inflammatory responses in microglia near Aβ-plaques may be driven by $Cu^{2+}$, potentially contributing to Aβ-plaque deposition and subsequent neuroinflammation.[17] Overall, $Cu^{2+}$ plays a significant role in oxidative stress, apoptosis, and neuroinflammation of AD cells. However, the specific mechanisms underlying its pathogenesis remain unclear.

Antioxidant protein 1 (ATOX1), initially discovered in yeast, protects cells from oxidative damage caused by superoxide and hydrogen peroxide.[18] It plays a key role in intracellular copper distribution. In healthy cells, ATOX1 delivers $Cu^{2+}$ to copper ATPases, including transmembrane P1B ATPase (ATP7B), located on the membrane of secretory vesicles and the trans Golgi apparatus network (TGN). As a copper chaperone, ATOX1 is essential for $Cu^{2+}$ secretion, facilitating its efflux from the cell.[19] Cells lacking ATOX1 exhibit compromised $Cu^{2+}$ efflux, leading to copper accumulation and eventual cell death.[20] Overexpression of ATOX1 enhances cellular antioxidant defenses in a copper-dependent manner.[18] However, the roles of ATOX1 in AD are still unclear.

This study investigated the role of ATOX1 in mitigating oxidative stress by reducing copper levels in microglia through ATP7B. In 5 × FAD mice, decreased ATOX1 expression was observed in microglia associated with Aβ-plaques. In BV2 cells treated with $A\beta_{1\text{-}42}$, ATOX1 interacted with ATP7B to facilitate the transfer of $Cu^{2+}$ to ATP7B. Overexpression of ATOX1 attenuated $Cu^{2+}$ accumulation and oxidative stress in microglia, ultimately decreasing cell apoptosis and neuroinflammation. This phenomenon may be due to a reduction in $Cu^{2+}$ levels following ATOX1 overexpression in microglia adjacent to Aβ-plaques, potentially serving as a protective mechanism in AD.

## Materials and methods

### Animals

In this study, C57BL/6 mice were hybridized to create 5 × FAD mice as the AD model. Five AD-related mutations were observed in 5 × FAD mice, with the model exhibiting significant Aβ-plaque deposition and cognitive impairment at 12 weeks.[21] Five mutations associated with AD have been identified in 5 × FAD mice, including the mutations in the human APP protein (Swedish type: K670N/M671L; Florida type: I716V; and London type: V717I) and mutations in the human PSEN1 protein (M146L and L286V).[22] In the study, male 5 × FAD transgenic mice were bred with female C57BL/6J mice. The progeny was separated from their mother and transitioned to solid food at around four weeks old, and genotype was determined using PCR analysis.[23] All 5 × FAD mice are transgenic heterozygotes. Throughout the experiment, due to known differences in disease progression between genders in the 5 × FAD mice, pathological differences related to amyloid plaques in the brain of 5-month-old male mice with 5 × FAD were evaluated, including cortical and hippocampus regions.[24] The mice were collectively placed in our specific pathogen-free facility and maintained under 12-h light and 12-h dark conditions, with free access to food and water. All procedures for this study were approved by the Animal Care and Use Committee of Chongqing Medical University (ID: IACUC-CQMU-2024-0626).

### Reagents and antibodies

The following antibodies were used: cluster of differentiation 68 (CD68), ionized calcium binding adaptor molecule 1 (IBA1), neuronal nuclei (NeuN), and glial fibrillary acidic protein (GFAP) were from Bio-Rad, Novus, Pronteintech, and Abcam, respectively. Antibodies against ATOX1 for immunofluorescence analysis were obtained from Pronteintech (26641-1-AP). ATOX1 and ATP7B antibodies used for Western blotting and co-immunoprecipitation analysis

were purchased from Santacruz (sc-100557, sc-373963). 1,1,1,3,3,3-hexafluoro-2-propanol (HFIP) was purchased from Sigma—Aldrich. $A\beta_{1-42}$ was purchased from Nanjing TG peptide. As previously mentioned, $A\beta_{1-42}$ was completely dissolved in HFIP using sonication. After dispensing the solution into appropriate volumes, the solvent was evaporated and the resultant $A\beta_{1-42}$ was stored at −80 °C before use.[25]

## Lentivirus preparation

ATOX1 overexpression lentivirus was constructed by Beijing Tsing Biological Company. The lentivirus was used to transfect the BV2 cell lines. Subsequently, purithromycin was used for drug screening to construct an ATOX1-OE stable transgenic BV2 cell line.

## BV2 cell culture conditions

The BV-2 cell line has undergone thorough characterization and was obtained from Shanghai Zhongqiao Xinzhou Biotechnology Co., LTD. The mouse microglial BV2 cell line was grown and routinely maintained in high-glucose Dulbecco's Modified Eagle Medium (DMEM) (Gibco) supplemented with 10% fetal bovine serum (Gibco) and 1% penicillin/streptomycin (Gibco), and cultured in a humidified 5% $CO_2$ atmosphere at 37 °C.

## Quantitative reverse transcription PCR

Total RNA of cultured cells and tissues was isolated using FastPure Cell/Tissue Total RNA Isolation Kit (Vazyme), and reverse-transcribed with the ABScript III RT Master Mix qPCR with gDNA Remover (ABclonal) according to the manufacturer's protocol. Real-time PCR was performed on the Biorad 96 Touch machine (Biorad) with 2 × Universal SYBR Green Fast qPCR Mix (ABclonal). β-actin was used as the internal control. The cycle threshold (Ct) of the gene transcript was standardized by the average Ct of housekeeping gene β-actin transcripts amplified in each reaction. The relative quantification of normalized transcript levels was calculated using the comparative Ct method ($^{\Delta\Delta}$Ct). The sequences of PCR primers for the genes examined are listed below: Forward (ATOX1): 5′- GGGAGGAGTGGAGTTCAACATTG-3′; Reverse (ATOX1): 3′- TGCCTCTTCAGTTTATATCCGGAA-5′; Forward (β-actin): 5′- AGTGTGACGTTGACATCCGTA -3′; Reverse (β-actin): 3′- GCCAGAGCAGTAATCTCCTTC-5′.

## Western blot analysis

Cultured cells or tissues were lysed in lysis buffer (RIPA, Pronteitech) containing phosphatase inhibitor Single-Use Cocktail (#1861281, Pronteitech). Subsequently, a probe-tip sonicator set at level 2 for 10 s (Fisher Scientific 550 Sonic Dismembrator) was used on ice, followed by centrifugation at 12,000 r.p.m at 4 °C for 16 min. The proteins were separated by polyacrylamide gel electrophoresis and transferred onto polyvinylidene difluoride membranes. The membranes were blocked with 5% nonfat dry milk in Tris-buffered saline-Tween solution at room temperature for 1 h and then incubated with antibodies overnight at 4 °C. After washing, secondary antibodies conjugated with horseradish peroxidase (Biosharp) were applied. For quantification, band intensities were normalized to β-actin and averaged from at least three independent experiments.

## Immunostaining, imaging, and quantification

To facilitate immunofluorescence staining of brain tissue, mice were anesthetized and perfused with cold phosphate-buffered saline through the heart to extract the right hemisphere of the brain. Subsequently, the brain specimens were fixed at 4 °C in a 4% paraformaldehyde solution overnight. Following fixation, the brains were immersed in a 30% sucrose solution at 4 °C until they reached a state of sinking. Coronal brain slices measuring 40 μm in thickness were then obtained using a sliding microtome with a freezing stage. The brain sections were washed three times with phosphate-buffered saline, followed by permeabilization and blocking in blocking buffer (1% bovine serum albumin and 0.1% Triton X-100 in phosphate-buffered saline) at room temperature for 1 h. Subsequently, the sections were incubated with primary antibodies in blocking buffer at 4 °C overnight. Following a series of washes, the secondary antibodies were added to the blocking buffer for 1 h. Then, the samples were washed and re-stained with dihydrochloride for 20 min. An Olympus confocal microscope was used for image acquisition. Image analysis was conducted utilizing a custom macro programmed within ImageJ software to quantify the staining of ATOX1-positive microglia. A standard threshold was chosen and uniformly applied to all channels of each image before measurement. The quantification of ATOX1 immunofluorescence involved normalizing the total area of ATOX1 immunofluorescence to the total area of IBA1 immunofluorescence.

## Measurement of copper level in cells

As mentioned above, the copper levels in BV2 cells were detected using a commercial copper colorimetric analysis kit (E-BC-K300-M, Elabscience).[26] The optical density was measured at the wavelength of 580 nm, and the copper concentration was calculated.

## Three-dimensional reconstruction

The 40 μm coronal slices were captured using an oil objective on a confocal microscope (Olympus). Imaging parameters were standardized for all experiments, and Z-stacking was conducted with 1.0 μm increments in the Z direction. Three-dimensional reconstruction of the selected images was carried out using Imaris 9.0.1 software (Bitplane).

## Detection of GSH, MDA, and SOD

Malondialdehyde (MDA), superoxide dismutase (SOD), and Glutathione (GSH) assay kits (BC0020, BC0170, BC1175, Solarbio) were used to detect intracellular MDA, SOD, and GSH levels according to the manufacturer's protocols. ImageJ software 1.26 was used for quantification.

### Identification of ATOX1 differentially expressed between the AD and normal samples

GSE33000, GSE48350, and GSE5281 microarray data were downloaded from the Gene Expression Omnibus (GEO) database (http://www.ncbi.nih.gov/geo). The raw data were downloaded as MINiML files. Box plots were drawn by GraphPad Prism 9.

### Statistical analysis and reproducibility

The statistical significance of the difference between the two groups was determined using the unpaired two-tailed Student's *t*-test or Mann–Whitney *U* test based on the normality test. The latest version of GraphPad Prism 9 (GraphPad Software) was used for statistics and graph images. No data were excluded from the analyses. All values were reported as mean ± standard error of the mean.

## Results

### ATOX1 decreased in AD

ATOX1, a key component of copper-transporting proteins, drew our attention. To explore its potential role in AD, we used the GEO database with "Alzheimer's disease" as the search term, selecting three large-scale datasets. First, we

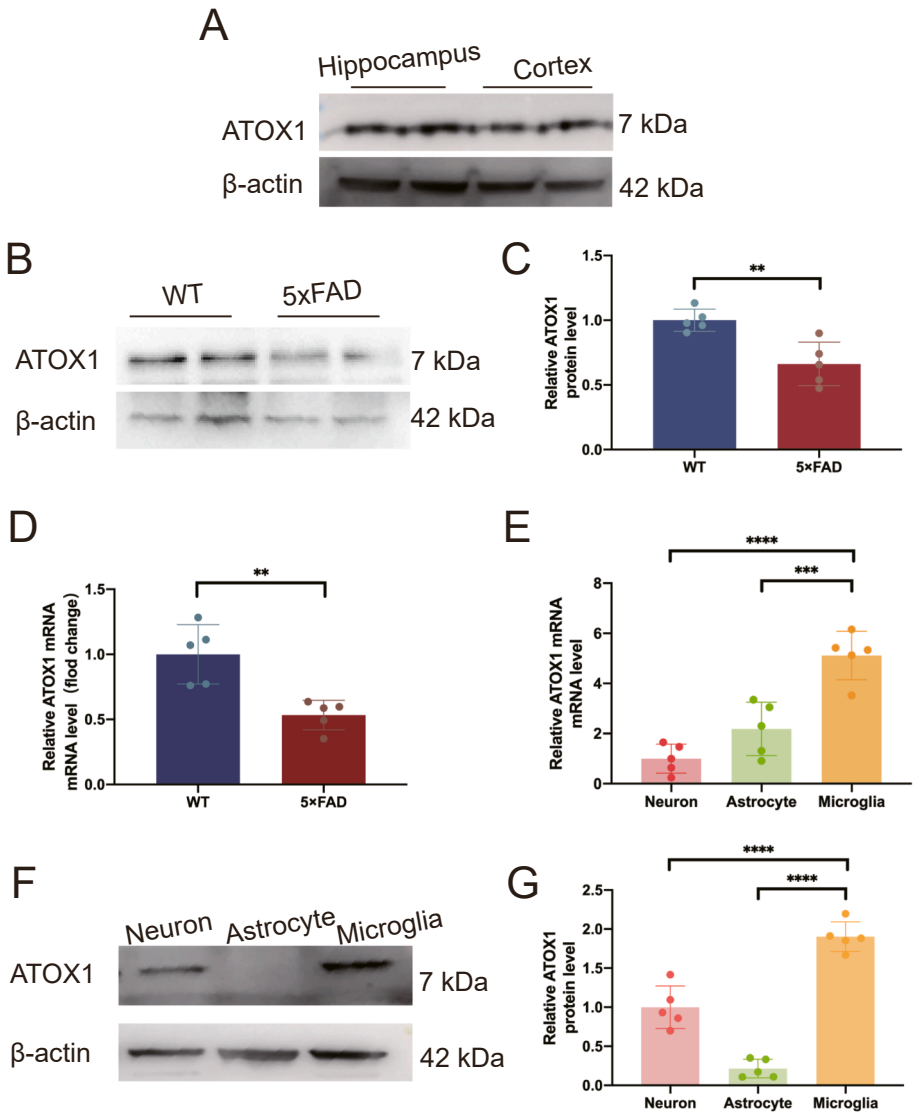


**Figure 1** Expression of ATOX1 in Alzheimer's disease. **(A)** Western blot analysis of ATOX1 protein levels in the cortical and hippocampal samples from 5-month-old C57BJ/L mice. **(B)** Western blot analysis of ATOX1 protein levels in the hippocampal samples from 5-month-old wild-type and 5 × FAD mice. **(C)** Quantifications of ATOX1 protein levels. **(D)** The mRNA levels of ATOX1 in wild-type and 5 × FAD mice were detected by real-time PCR. $^{**}p < 0.01$; *t*-test and Tukey's post hoc analysis. **(E)** Quantifications of ATOX1 mRNA levels in neurons, astrocytes, and microglia. **(F)** The ATOX1 protein levels in neurons, astrocytes, and microglia were detected by Western blot analysis. **(G)** Quantifications of ATOX1 protein levels. $^{***}p < 0.001$, $^{****}p < 0.0001$; data were reported as mean ± standard error of the mean; one-way ANOVA with Tukey's post hoc analysis.

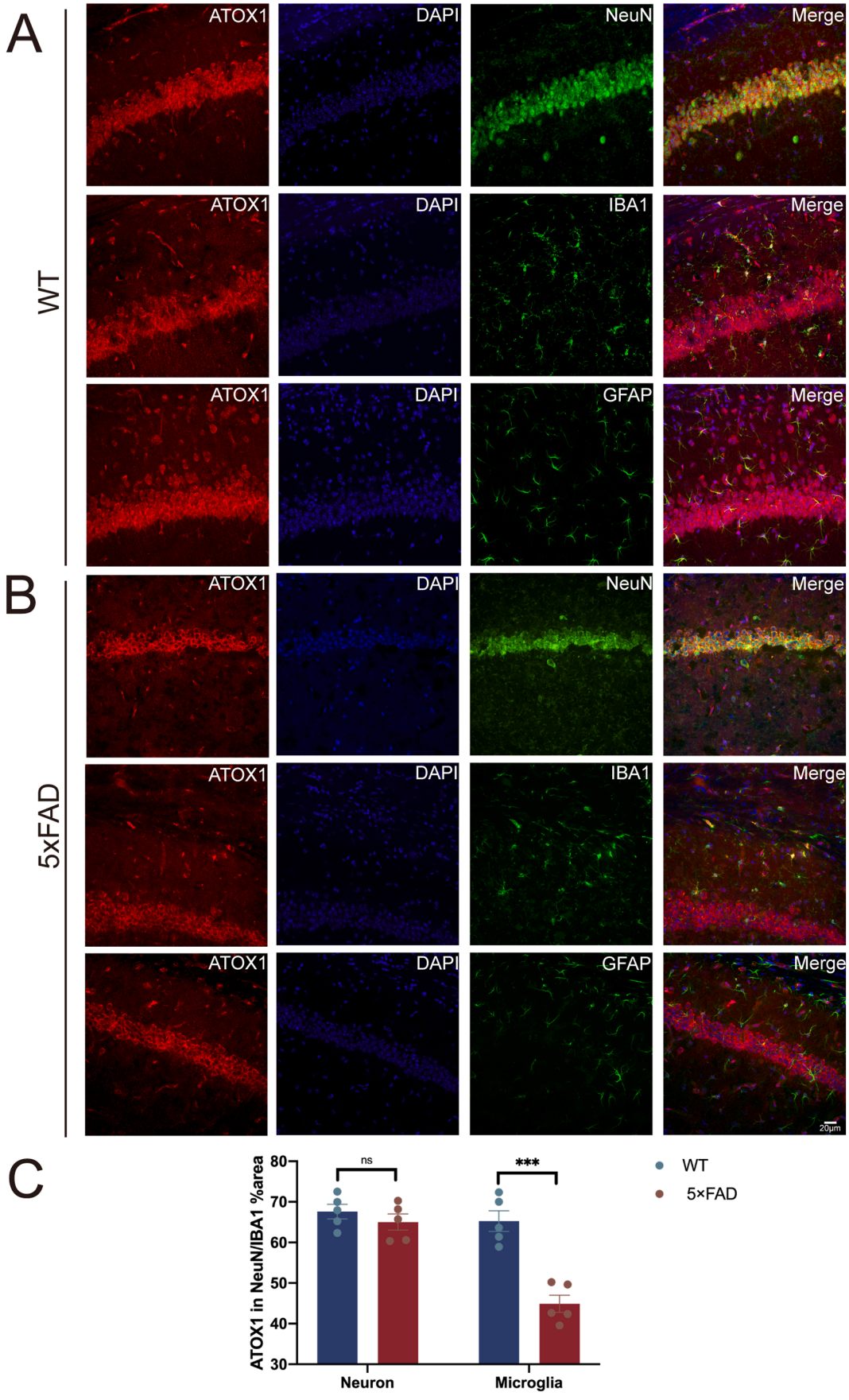
A
WT
ATOX1
DAPI
NeuN
Merge
ATOX1
DAPI
IBA1
Merge
ATOX1
DAPI
GFAP
Merge
B
5xFAD
ATOX1
DAPI
NeuN
Merge
ATOX1
DAPI
IBA1
Merge
ATOX1
DAPI
GFAP
Merge
20μm
C
ATOX1 in NeuN/IBA1 %area
80
70
60
50
40
30
ns
***
Neuron
Microglia
WT
5×FAD

analyzed that the mRNA expression of ATOX1 decreased in an AD patient (Fig. S1A–S1C).

Previous studies have documented the expression of ATOX1 in rodent brains, particularly in the hippocampus and cortex.[27] The 5 × FAD transgenic mice employed in this study were generated on a C57BL/6 genetic background. Firstly, we confirmed ATOX1 presence in both the hippocampus and parietal cortex of C57BL/6 (Fig. 1A). The bilateral hippocampal tissues from 5-month-old 5 × FAD mice were then analyzed, revealing a significant down-regulation of ATOX1 expression compared with age-matched wild-type controls ($p = 0.0015$, $p = 0.0046$; Fig. 1B–D). To determine cell-type specificity of ATOX1 expression in the central nervous system, we quantified its levels in primary neurons, astrocytes, and microglia. Notably, ATOX1 was expressed in both neurons and microglia, with the highest abundance in microglia ($p = 0.0002$, $p = 0.02$; Fig. 1E–G). While prior reports confirmed ATOX1 presence in the central nervous system, its hippocampal distribution remained incompletely characterized.[28,29]

Immunofluorescence co-localization studies revealed ATOX1 expression in both neurons and microglia within the hippocampal region (Fig. 2A). However, ATOX1 fluorescence intensity was selectively diminished in microglia of 5 × FAD mice, while the expression in neurons remained unchanged (Fig. 2B and C; $p = 0.0003$ in microglia; $p > 0.05$ in neurons).

## ATOX1 was expressed in Aβ-plaque-associated microglia in AD

Microglia are typically in a resting state. Under pathological conditions, such as Aβ-plaques, microglia become activated and localize around to Aβ before phagocytosing them.[30,31] These microglia are referred to as plaque-associated microglia. First, immunofluorescence was used to examine the association between $ATOX1^+$ microglia and Aβ-plaques in the hippocampus and cortex of 5 × FAD mice. Notably, most $ATOX1^+$ microglia were located around $IBA1^+$ microglia surrounding Aβ-plaques (Fig. 3A). Three-dimensional reconstruction confirmed the co-localization of $ATOX1^+$ microglia and Aβ-plaques (Fig. 3B). Additionally, we observed lower expression of ATOX1 in non-plaque-associated microglia (Fig. S2A and S2B; $p = 0.0172$).

In AD, CD68-labeled lysosomes are crucial for the phagocytosis of Aβ-plaques by microglia. $CD68^+$ microglia are considered key for clearing Aβ.[32–34] The results demonstrated a high degree of co-localization between the phagocytic marker CD68 and ATOX1 in 5 × FAD mice, suggesting that ATOX1-positive microglia may possess enhanced phagocytic activity (Fig. 3C). Further immunofluorescence analysis revealed significant overlap between CD68 and ATOX1 in $IBA1^+$ microglia near Aβ-plaques (Fig. 3D), indicating that ATOX1 may influence microglial phagocytic function in AD pathology. The co-localization in AD suggests ATOX1 involvement in microglial activation. The observed Aβ-plaque-associated co-localization further implies the potential role of ATOX1 in regulating phagocytic function.

## ATOX1 reduced copper overload in BV2 cells through ATP7B

ATOX1 is the primary copper chaperone in the cytoplasm. To investigate its role, we conducted semi-quantitative analysis using immunofluorescence. After treating BV2 cells with $A\beta_{1\text{-}42}$, we observed a significant reduction in ATOX1 expression (Fig. 4A and B; $p = 0.003$).

Previous studies have shown that ATP7B plays a role in removing excess copper from the plasma membrane of cells.[35–37] Based on these findings, we hypothesized that ATOX1 might function through ATP7B in BV2 cells. To test this hypothesis, we extracted cellular proteins after $A\beta_{1\text{-}42}$ treatment and detected a significant increase in ATP7B expression in the $A\beta_{1\text{-}42}$ group (Fig. 5A and B; $p = 0.0002$). To further explore the relationship between ATOX1 and ATP7B, co-immunoprecipitation confirmed their interaction (Fig. 5C). Additionally, immunofluorescence triple-labeling experiments performed on the brains of wild-type and 5 × FAD mice demonstrated clear co-localization of IBA1, ATOX1, and ATP7B in the hippocampus (Fig. 5D and E; $p = 0.0053$, $p = 0.0013$).

To explore whether ATOX1 activation affects copper accumulation via ATP7B, a lentivirus was used to overexpress ATOX1 in BV2 cells. Overexpression efficiency was found to be 63% (Fig. 6A and B; $p = 0.0171$). Further results revealed copper accumulation in BV2 cells following $A\beta_{1\text{-}42}$ treatment (Fig. 6C; $p = 0.0125$). In contrast, overexpression of ATOX1 led to a significant reduction in intracellular copper concentrations ($p < 0.0001$; Fig. 6C). These findings suggest that ATOX1 regulates $Cu^{2+}$ concentrations in microglia through its interaction with ATP7B, and that changes in ATOX1 expression are associated with $Cu^{2+}$ accumulation in these cells.

## ATOX1 upregulation reduces oxidative stress, apoptosis, and neuroinflammation

The increase of $Cu^{2+}$ in BV2 cells induced by $A\beta_{1\text{-}42}$ requires many adaptive changes in the cells to prevent the toxicity from ROS. Next, the levels of antioxidants that protect cells from $Cu^{2+}$ induced oxidative stress were tested. GSH has the capability to bind to a majority of cytoplasmic $Cu^{2+}$, thereby promoting cell adaptation to elevated $Cu^{2+}$ concentrations and mitigating resultant oxidative stress.[38,39] The study observed a significant decrease in GSH expression in BV2 cells after $A\beta_{1\text{-}42}$ treatment ($p = 0.0033$; Fig. 7A). After overexpression of ATOX1 and treatment with $A\beta_{1\text{-}42}$, GSH increased compared with the NC-$A\beta_{1\text{-}42}$ group (Fig. 7A; $p = 0.0043$). In the SOD activity assay, similar findings were observed in both the NC and NC-$A\beta_{1\text{-}42}$ groups (Fig. 7B;

**Figure 2** Cellular localization of ATOX1 in wild-type and AD mice. **(A)** Immunofluorescent staining of ATOX1 (red) and neuronal nuclei (NeuN)/ionized calcium binding adapter molecule 1 (IBA1)/glial fibrillary acidic protein (GFAP) (green) in the hippocampus from wild-type mice. **(B)** Immunofluorescent staining of ATOX1 (red) and NeuN, IBA1, and GFAP (green) in the hippocampus from 5-month-old male 5 × FAD mice. $n = 5$ in each group. Scale bar: 20 μm. **(C)** Quantification of ATOX1 intensity in neurons and microglia. $^{ns}P > 0.05$, $^{***}p < 0.001$; data were reported as mean ± standard error of the mean; *t*-test and Tukey's post hoc analysis.

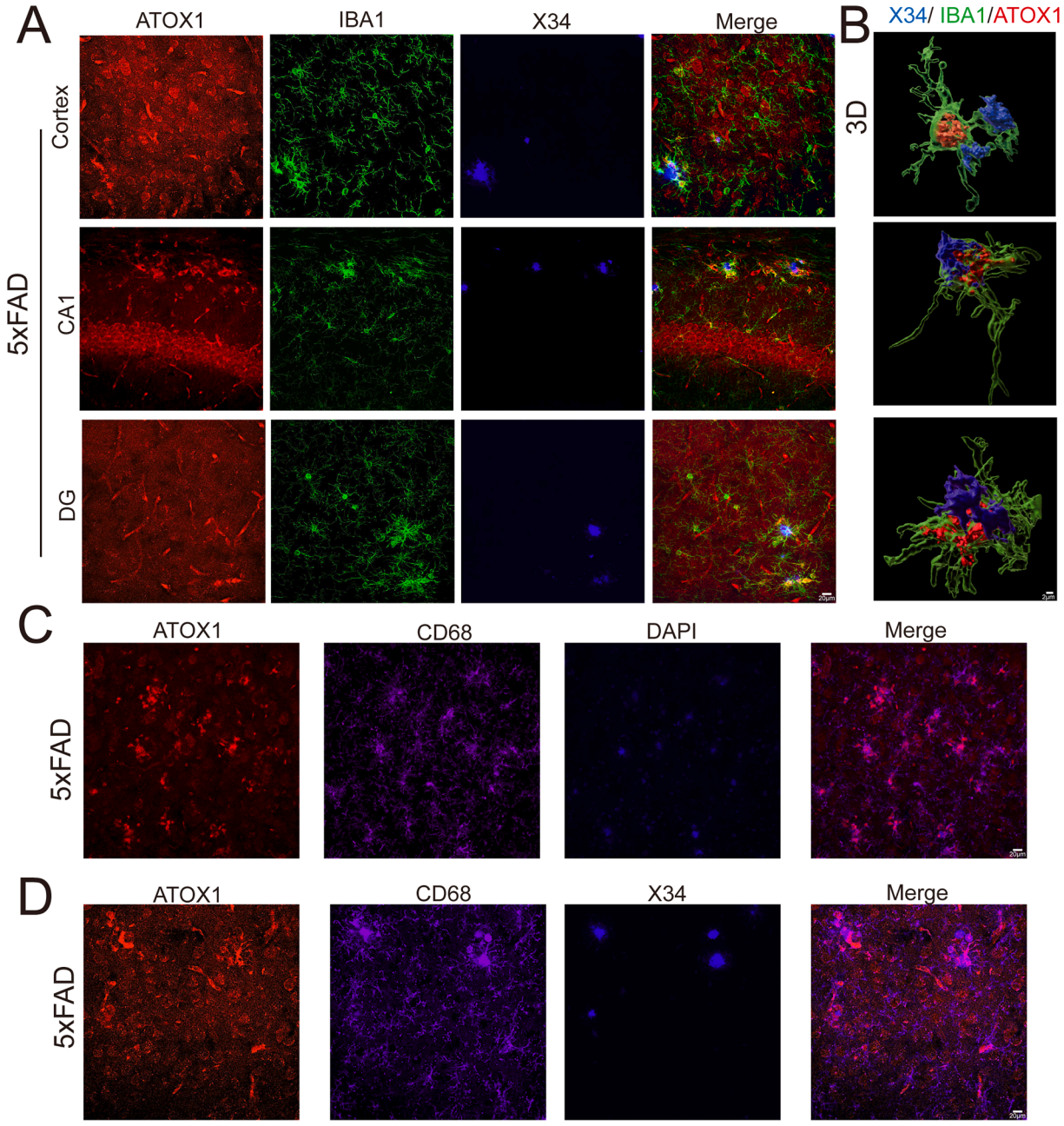


**Figure 3** ATOX1 decreased in Aβ-plaque-associated microglia in AD. **(A)** Immunofluorescent staining of ATOX1 (red), X34 (blue), and IBA1 (green) in the hippocampus from 5-month-old 5 × FAD mice. Scale bar: 20 μm. **(B)** Representative three-dimensional images reconstruction after immunofluorescence triple labeling of ATOX1 (red), X34 (blue), and IBA1 (green) in hippocampal regions from 5-month-old 5 × FAD mice. Scale bar: 5 μm. **(C)** Double immunofluorescent staining of ATOX1 (red) and CD68 (magenta) from 5-month-old 5 × FAD mice. **(D)** Immunofluorescent staining of ATOX1 (red), X34 (blue), and CD68 (magenta) from 5-month-old 5 × FAD mice. Scale bar: 20 μm.

$p < 0.0001$). Although no statistically significant difference was found between the OE-A$\beta_{1\text{-}42}$ and NC-A$\beta_{1\text{-}42}$ groups, an increase in SOD level was still observed (Fig. 7B; $p > 0.05$). It is also worth noting that the oxidative stress indicator MDA content was significantly reduced in the OE-A$\beta_{1\text{-}42}$ group (Fig. 7C; $p = 0.0006$).

Previous studies have reported that excessive exposure to $Cu^{2+}$ may lead to cell apoptosis.[11] As shown in Figure 7D–I, compared with the NC group, A$\beta_{1\text{-}42}$ significantly decreased the protein level of Bcl2 (Fig. 7D and E; $p = 0.0402$) and increased the protein level of Bax (Fig. 7F and G; $p = 0.0105$), and cleaved caspase 3 (Fig. 7H and I; $p = 0.0088$). In addition, compared with the NC-A$\beta_{1\text{-}42}$ group, the protein levels of cleaved caspase 3 in BV2 microglia were significantly lower in the OE-A$\beta_{1\text{-}42}$ group (Fig. 7H and I; $p = 0.00391$), but Bcl2 protein levels increased (Fig. 7D and E; $p = 0.0055$). Although the protein expression of Bax did not show statistical significance in the NC-A$\beta_{1\text{-}42}$ and OE-A$\beta_{1\text{-}42}$ groups, a decrease in Bax expression was observed in the OE-A$\beta_{1\text{-}42}$ group (Fig. 7F and G;

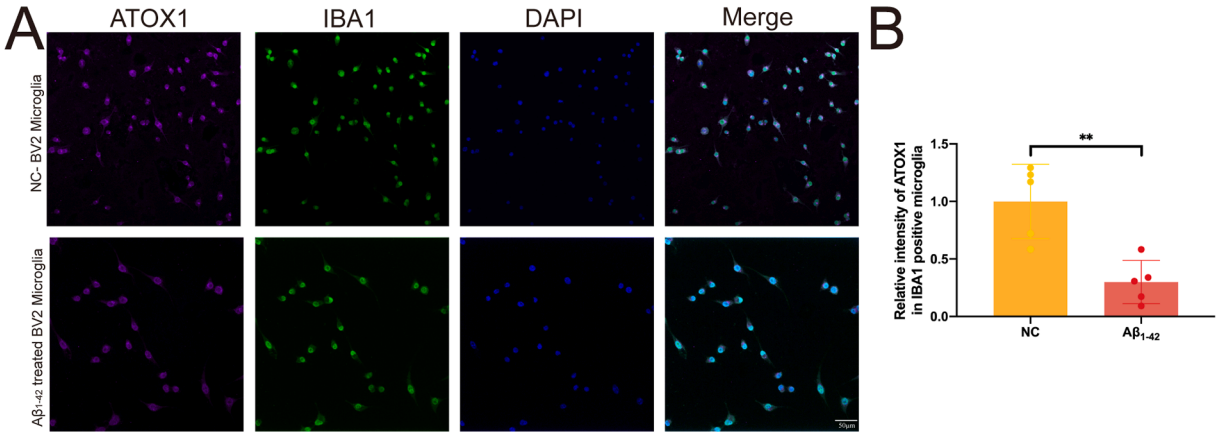


**Figure 4** ATOX1 is reduced in $A\beta_{1\text{-}42}$-treated BV2 cells. **(A)** Immunofluorescence analysis of ATOX1 (red) and IBA1 (green) in BV2 microglia with or without $A\beta_{1\text{-}42}$. $^{**}p < 0.01$; data were reported as mean ± standard error of the mean; *t*-test and Tukey's post hoc analysis.

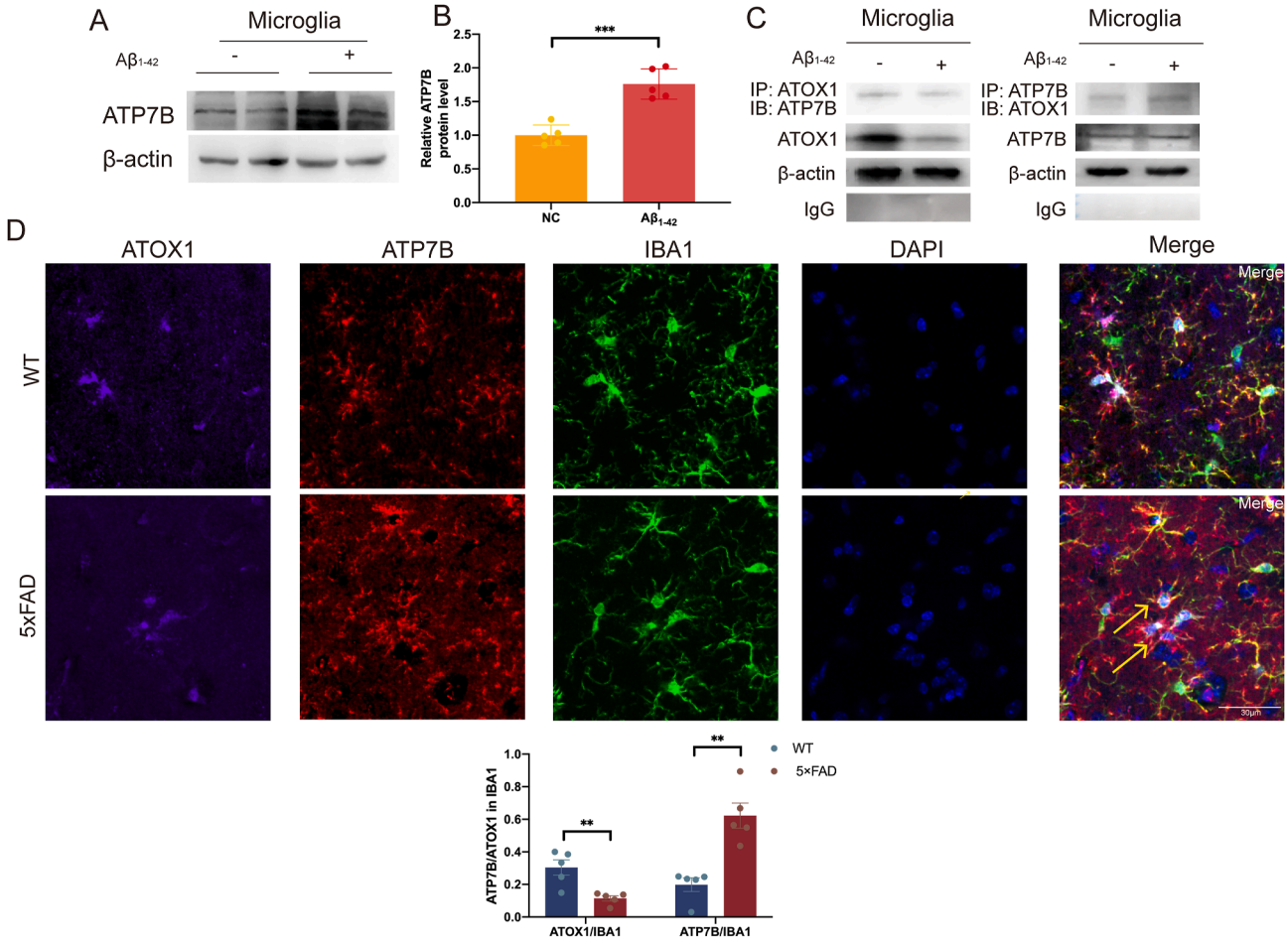


**Figure 5** ATOX1 exerts a functional role in AD through interaction with ATP7B. **(A, B)** Expression of the main copper export protein ATP7B was detected in BV2 microglia with or without $A\beta_{1\text{-}42}$ by Western blot analysis. ATP7B protein levels were quantified. **(C)** Detection of the interaction of ATOX1 and ATP7B on BV2 microglia cells treated with $A\beta_{1\text{-}42}$ by co-immunoprecipitation. **(D)** Immunofluorescent staining of ATOX1 (magenta), ATP7B (red), IBA1 (green), and DAPI (blue) in the brain from 5-month-old wild-type and 5 × FAD mice. Scale bar: 30 μm. **(E)** Quantification of ATOX1 and ATP7B intensity in microglia. $^{**}p < 0.01$, $^{***}p < 0.001$; data were reported as mean ± standard error of the mean; *t*-test and Tukey's post hoc analysis.

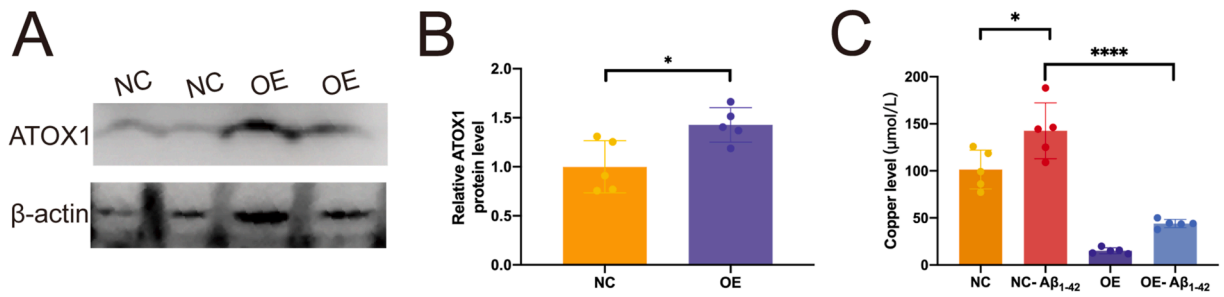


**Figure 6** ATOX1 reduces copper overload in BV2 cells. **(A, B)** Lentivirus (LV) was used to mediate stable ATOX1 overexpression (OE). ATOX1 protein levels in BV2 cells with or without LV-OE were quantified. *$p < 0.05$; data were reported as mean ± standard error of the mean; *t*-test and Tukey's post hoc analysis. **(C)** The copper level in NC and OE in BV2 microglia with or without $A\beta^{1\text{-}42}$. *$p < 0.05$, ****$p < 0.0001$; data were reported as mean ± standard error of the mean; one-way ANOVA analysis followed by Tukey's multiple comparison test.

$p > 0.05$). In summary, these findings indicate that the level of $Cu^{2+}$ increases after $A\beta_{1\text{-}42}$ treatment, while excessive $Cu^{2+}$ leads to cellular oxidative stress and induces BV2 apoptosis. Overexpression of ATOX1 can save this neurotoxicity. This indicates that ATOX1 can alleviate oxidative stress and cell apoptosis in microglia in AD.

The elevation of $Cu^{2+}$ concentration results in a disruption of metal homeostasis, subsequently inducing the generation of ROS and perturbation of the inflammatory equilibrium.[40] The synthesis of pro-inflammatory cytokines plays a role in neuroinflammation and contributes to the progression of AD.[41] Our research centers on the multifunctional interleukin (IL)-1β and IL-6, which have been previously linked to inflammatory reactions in microglia in AD.[42] Using an ELISA on BV2 cells, compared with the NC group, in the NC-$A\beta_{1\text{-}42}$ group, the levels of IL-1β and IL-6 significantly increased (Fig. 7J and K; $p < 0.0001$). The levels of cytokines IL-1β and IL-6 significantly decreased in the AD model with ATOX1 overexpression (OE-$A\beta_{1\text{-}42}$ group) (Fig. 7J and K; $p < 0.0001$). These results indicate that overexpression of ATOX1 can inhibit pro-inflammatory responses.

## Discussion

This study demonstrates that ATOX1 expression is markedly reduced in microglia in 5 × FAD cells. Notably, ATOX1 expression is reduced in Aβ-plaque-associated microglia compared with microglia. ATOX1 plays a critical role in maintaining $Cu^{2+}$ homeostasis via ATP7B. Modulating ATOX1 expression alleviates oxidative stress, inhibits apoptosis, and reduces neuroinflammation in microglia. The relationship between microglial cell death and the improvement of AD pathology is complex. Microglia play multiple roles in AD, including neuron protection and clearance of pathological substances. However, excessive activation can trigger inflammation and exacerbate neuronal damage. In this study, we found that the compensatory addition of ATOX1 may have protective effects. It alleviates oxidative stress while reducing the negative impact of apoptosis and inflammation. This balance may help improve AD pathology. To our knowledge, this is the first study to demonstrate that ATOX1 provides neuroprotection in AD by preserving copper homeostasis in microglia.

Previous studies have shown that high concentrations of $Cu^{2+}$ accumulate near Aβ-plaques in AD brain 43. In fact, some data from the AD mouse model indicate that $Cu^{2+}$ chelation reduces Aβ-plaque deposition and improves cognitive function.[44] ATOX1, a key cytoplasmic copper transporter, plays a crucial role in $Cu^{2+}$ homeostasis. A study has found that ATPase is highly expressed in $Cu^{2+}$-overloaded microglia and mediates $Cu^{2+}$ transport.[45] In cells, $Cu^{2+}$ is transferred to ATP7B, located in the trans-Golgi network and inner vesicles, via ATOX1, and subsequently exported to the extracellular space by ATP7B. ATOX1 is essential for regulating cellular $Cu^{2+}$ levels through this pathway.[45,46] In this study, ATOX1 and ATP7B interacted in BV2 cells treated with $A\beta_{1\text{-}42}$. Furthermore, ATP7B expression was up-regulated, while ATOX1 expression was down-regulated. These changes may contribute to the increased $Cu^{2+}$ level in microglia. After ATOX1 loss, $Cu^{2+}$ accumulation in the cytoplasm was directly observed.[47] Our research showed that ATOX1 up-regulation reduced $Cu^{2+}$ overload in microglia. The results suggest that the regulation of $Cu^{2+}$ transport by ATOX1 and ATP7B may help maintain $Cu^{2+}$ homeostasis in activated microglia at Aβ-plaque sites.

The bonding of $Cu^{2+}$ to Aβ forms a stable complex, leading to increased ROS production in mouse brain tissue. High concentrations of $Cu^{2+}$ can disrupt the oxidation/antioxidation balance in the brain tissue of AD patients, leading to ROS accumulation and oxidative stress damage.[47] Cells use a variety of antioxidant systems to mitigate oxidative stress, including free radical scavenging enzymes and non-enzymatic antioxidants. SOD is considered the most important enzyme in combating ROS, as it catalyzes the conversion of superoxide into water and oxygen. MDA, a byproduct of lipid oxidation, exacerbates cellular membrane damage, making it a key indicator of membrane integrity. GSH, a low-molecular-weight scavenger, binds to most cytoplasmic $Cu^{2+}$, enabling cells to tolerate high $Cu^{2+}$ levels while mitigating oxidative damage.[38] These molecules classically participate in the oxidation/antioxidant balance. Essential antioxidants are crucial in eliminating free radicals and maintaining redox equilibrium. Studies have shown that overexpression of ATOX1 can reduce MDA levels and increase GSH levels in BV2 cells stimulated by $A\beta_{1\text{-}42}$, thereby enhancing their antioxidant capacity. This suggests that ATOX1 up-regulation may protect cells from

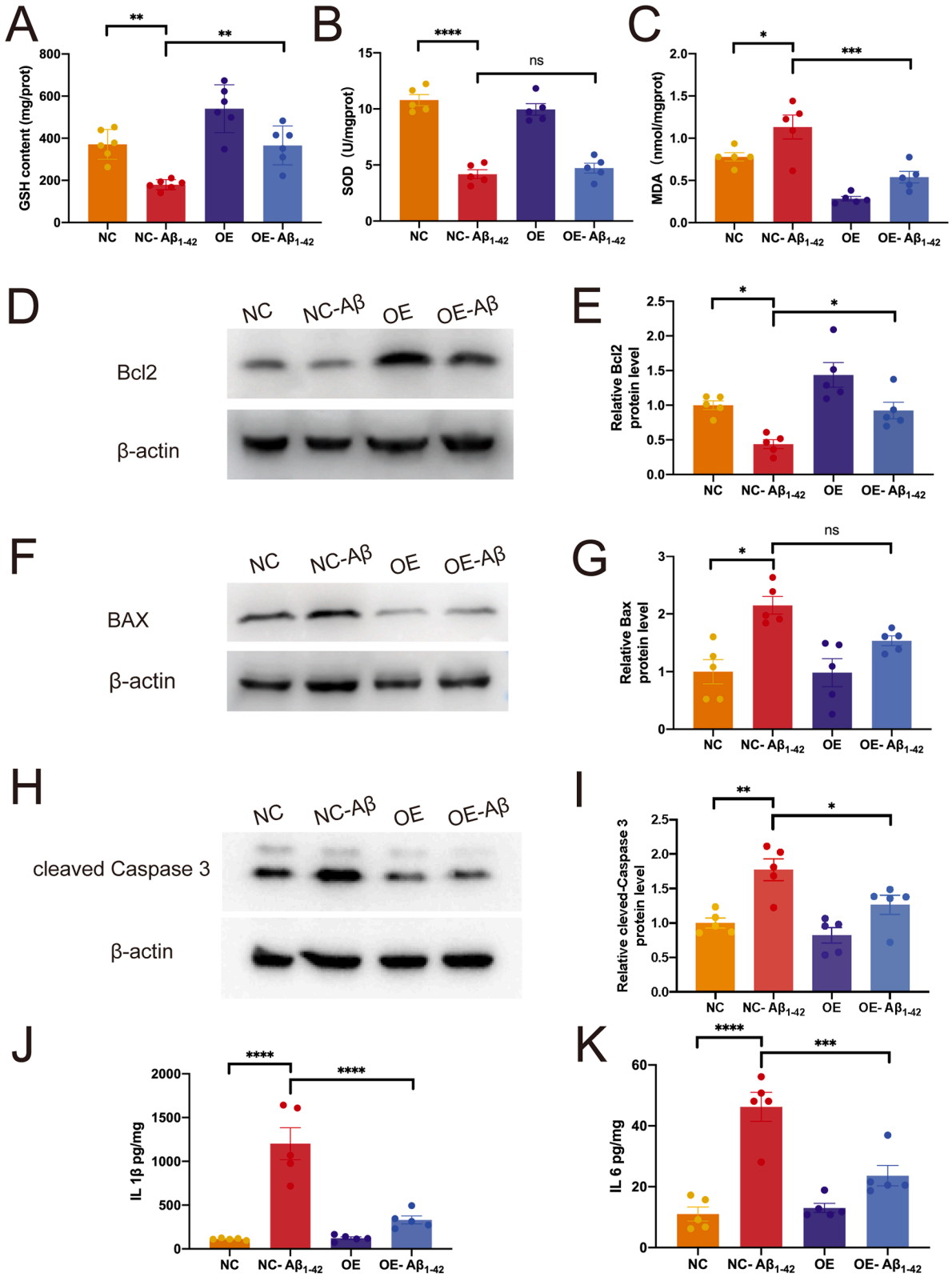


**Figure 7** The up-regulation of ATOX1 attenuates oxidative stress, apoptosis, and neuroinflammation in BV2 cells. **(A—C)** Expression levels of antioxidants, superoxide dismutase (SOD), glutathione (GSH), and malondialdehyde (MDA), were measured in comparison to NC-BV2. **(D—I)** Western blot analysis was used to measure Bcl2, BAX, and cleaved caspase 3 expression in lentivirus-treated BV2 microglia with or without $A\beta_{1\text{-}42}$. Quantifications of protein levels are shown in E, G, I. **(M, N)** The IL-1β and IL-6 levels in lentivirus-treated BV2 microglia with or without $A\beta_{1\text{-}42}$ were measured by ELISA. $^{ns}P > 0.05$, $^{*}p < 0.05$, $^{**}p < 0.01$, $^{***}p < 0.001$, $^{****}p < 0.0001$; data were reported as mean ± standard error of the mean; one-way ANOVA analysis followed by Tukey's multiple comparison test.

oxidative stress by enhancing GSH levels. Previous research has shown that ATOX1 up-regulation can alleviate $Cu^{2+}$-induced oxidative stress in neurons by reducing ROS levels.[48] However, the exact protective mechanism of ATOX1 in AD remains unclear.

Oxidative stress is a key factor in inducing programmed cell death, specifically apoptosis, and neuroinflammation in microglia.[49,50] Numerous studies have demonstrated a strong association between excessive microglia activation and oxidative stress.[51–53] This hyperactivation not only facilitates the release of pro-inflammatory cytokines, but also triggers microglial apoptosis and dysfunction, thereby impairing the innate immune functions of the brain 54,55. It is suggested that oxidative stress may act as an indirect contributor to $Cu^{2+}$ overload. The Bcl2 protein family plays a central role in regulating anti-apoptotic processes. Upon receiving apoptotic signals, Bcl2 family proteins will transfer from the cytoplasm to the mitochondrial membrane, where they exert anti-apoptotic effects. The ratio of Bcl2 to Bax is critical in determining whether a cell survives or undergoes apoptosis.[56] Additionally, mitochondrial oxidative phosphorylation can release apoptosis-inducing factors into the cytoplasm, activating caspase-3 and further promoting apoptosis.[57] Our findings showed that *in vitro*, Bcl2 expression was significantly decreased while pro-apoptotic proteins, including Bax and cleaved-caspase 3, were markedly increased, indicating a high rate of apoptosis. Conversely, overexpression of ATOX1 reversed these changes, suggesting a potential protective mechanism against apoptosis and oxidative damage. These findings support the potential of exogenous ATOX1 to reduce apoptosis in AD. In summary, our findings offer initial support for the potential protective role of ATOX1 in modulating microglial function in the context of AD. A previous study has suggested a link between microglial resistance to apoptosis and chronic inflammation.[58] Furthermore, microglia can promote apoptosis through the release of various pro-inflammatory factors.[59] The results show that the up-regulation of ATOX1 inhibits the expression of IL-1β and IL-6, thereby reducing inflammation. Those findings suggest that ATOX1 may help mitigate neuroinflammation in AD models. Consequently, investigating the role of ATOX1 in controlling AD has sparked interest due to its potential therapeutic implications.

Preliminary results indicate that ATOX1 is localized in both microglia and neurons. Since ATOX1 is predominantly expressed in microglia, subsequent *in vitro* experiments focused on its effects in these cells. Clarifying the role of ATOX1 in microglial function is essential in the context of AD. This study is the first to identify a potential association between ATOX1 and Aβ-plaque-associated microglia, possibly linked to $Cu^{2+}$ regulation and antioxidant activity. Additionally, up-regulation of ATOX1 effectively protects microglia from oxidative stress damage, consequently reducing the incidence of apoptosis and neuroinflammation. A previous study has demonstrated that elevated $Cu^{2+}$ levels can intensify oxidative stress-induced microglial apoptosis in an AD mouse model.[60] This current finding suggests that ATOX1 may lower intracellular $Cu^{2+}$ levels by modulating microglial activity. However, further studies are needed to clarify the mechanisms through which ATOX1 influences microglial function and contributes to AD pathogenesis.

## Conclusion

ATOX1 serves as a key link between $Cu^{2+}$ and microglia in AD. The up-regulation of ATOX1 demonstrates a protective influence on microglia in AD, suggesting potential therapeutic avenues for addressing the pathogenesis of the condition.

## CRediT authorship contribution statement

**Fuxin Zhong:** Writing — original draft, Resources, Conceptualization. **Jiani Wu:** Supervision, Conceptualization. **Zhangjing Deng:** Methodology. **Wuhan Yu:** Formal analysis. **Jiaqi Song:** Supervision. **Yingxi Chen:** Visualization. **Weihua Yu:** Visualization, Supervision. **Yang Lü:** Writing — review & editing, Visualization.

## Ethics declaration

The study protocol was approved by the Ethics Committee of Chongqing Medical University. All animal studies were conducted in accordance with the principles outlined in the Animal Research: Reporting In Vivo Experiments guidelines.

## Data availability

The datasets used and/or analyzed during the current study are available from the corresponding author upon reasonable request. The raw data supporting the conclusions of this article will be made available by the authors without undue reservation.

## Conflict of interests

The authors declared no competing interests.

## Funding

This study was supported by grants from the Chongqing Talent Plan (China) (No. cstc2022ycjh-bgzxm0184), the Key Project of Science and Technology Research Program of Chongqing Municipal Education Commission (China) (No. KJZD-K202200405), the Innovation Project for Doctoral Students at The First Affiliated Hospital of Chongqing Medical University (China) (No. CYYY-BSYJSCXXM-202320), and the Chongqing Medical Key Discipline and Regional Medical Key Discipline Development Project (China) (0201 [2023] No. 160 202412).

## Appendix A. Supplementary data

Supplementary data to this article can be found online at https://doi.org/10.1016/j.gendis.2025.101888.

## References


1. Holtzman DM, Morris JC, Goate AM. Alzheimer's disease: the challenge of the second century. *Sci Transl Med*. 2011;3(77):77sr1.
2. Hardy J, Selkoe DJ. The amyloid hypothesis of Alzheimer's disease: progress and problems on the road to therapeutics. *Science*. 2002;297(5580):353—356.
3. Dong J, Canfield JM, Mehta AK, et al. Engineering metal ion coordination to regulate amyloid fibril assembly and toxicity. *Proc Natl Acad Sci U S A*. 2007;104(33):13313—13318.
4. Barnham KJ, Haeffner F, Ciccotosto GD, et al. Tyrosine gated electron transfer is key to the toxic mechanism of Alzheimer's disease β-amyloid. *FASEB J*. 2004;18(12):1427—1429.
5. Sayre LM, Perry G, Harris PL, Liu Y, Schubert KA, Smith MA. *In situ* oxidative catalysis by neurofibrillary tangles and senile plaques in Alzheimer's disease: a central role for bound transition metals. *J Neurochem*. 2000;74(1):270—279.
6. Miller LM, Wang Q, Telivala TP, Smith RJ, Lanzirotti A, Miklossy J. Synchrotron-based infrared and X-ray imaging shows focalized accumulation of Cu and Zn co-localized with beta-amyloid deposits in Alzheimer's disease. *J Struct Biol*. 2006;155(1):30—37.
7. Hickey JL, Lim S, Hayne DJ, et al. Diagnostic imaging agents for Alzheimer's disease: copper radiopharmaceuticals that target aβ plaques. *J Am Chem Soc*. 2013;135(43):16120—16132.
8. Schino I, Cantore M, de Candia M, et al. Exploring mannosylpurines as copper chelators and cholinesterase inhibitors with potential for Alzheimer's disease. *Pharmaceuticals (Basel)*. 2023;16(1):54.
9. Song XB, Liu G, Liu F, et al. Autophagy blockade and lysosomal membrane permeabilization contribute to lead-induced nephrotoxicity in primary rat proximal tubular cells. *Cell Death Dis*. 2017;8(6):e2863.
10. Erboga M, Kanter M, Aktas C, et al. Thymoquinone ameliorates cadmium-induced nephrotoxicity, apoptosis, and oxidative stress in rats is based on its anti-apoptotic and anti-oxidant properties. *Biol Trace Elem Res*. 2016;170(1):165—172.
11. Sun Y, Liu C, Liu Y, Hosokawa T, Saito T, Kurasaki M. Changes in the expression of epigenetic factors during copper-induced apoptosis in PC12 cells. *J Environ Sci Health A Tox Hazard Subst Environ Eng*. 2014;49(9):1023—1028.
12. Spincemaille P, Chandhok G, Newcomb B, et al. The plant decapeptide OSIP108 prevents copper-induced apoptosis in yeast and human cells. *Biochim Biophys Acta*. 2014;1843(6):1207—1215.
13. Indo HP, Davidson M, Yen HC, et al. Evidence of ROS generation by mitochondria in cells with impaired electron transport chain and mitochondrial DNA damage. *Mitochondrion*. 2007;7(1—2):106—118.
14. Siddiqui MA, Alhadlaq HA, Ahmad J, Al-Khedhairy AA, Musarrat J, Ahamed M. Copper oxide nanoparticles induced mitochondria mediated apoptosis in human hepatocarcinoma cells. *PLoS One*. 2013;8(8):e69534.
15. Shang YC, Chong ZZ, Wang S, Maiese K. Prevention of β-amyloid degeneration of microglia by erythropoietin depends on Wnt1, the PI 3-K/mTOR pathway, bad, and Bcl-xL. *Aging*. 2012;4(3):187—201.
16. Zhu N, Lin J, Wang K, Wei M, Chen Q, Wang Y. Huperzine A protects neural stem cells against Aβ-induced apoptosis in a neural stem cells and microglia co-culture system. *Int J Clin Exp Pathol*. 2015;8(6):6425—6433.
17. Haage V, De Jager PL. Neuroimmune contributions to Alzheimer's disease: a focus on human data. *Mol Psychiatry*. 2022;27(8):3164—3181.
18. Lin SJ, Culotta VC. The ATX1 gene of *Saccharomyces cerevisiae* encodes a small metal homeostasis factor that protects cells against reactive oxygen toxicity. *Proc Natl Acad Sci U S A*. 1995;92(9):3784—3788.
19. Lasorsa A, Nardella MI, Rosato A, et al. Mechanistic and structural basis for inhibition of copper trafficking by platinum anticancer drugs. *J Am Chem Soc*. 2019;141(30):12109—12120.
20. Hamza I, Prohaska J, Gitlin JD. Essential role for Atox1 in the copper-mediated intracellular trafficking of the Menkes ATPase. *Proc Natl Acad Sci U S A*. 2003;100(3):1215—1220.
21. Neuner SM, Heuer SE, Huentelman MJ, O'Connell KMS, Kaczorowski CC. Harnessing genetic complexity to enhance translatability of Alzheimer's disease mouse models: a path toward precision medicine. *Neuron*. 2019;101(3):399—411.e5.
22. Oakley H, Cole SL, Logan S, et al. Intraneuronal beta-amyloid aggregates, neurodegeneration, and neuron loss in transgenic mice with five familial Alzheimer's disease mutations: potential factors in amyloid plaque formation. *J Neurosci*. 2006;26(40):10129—10140.
23. Boeddrich A, Haenig C, Neuendorf N, et al. A proteomics analysis of 5xFAD mouse brain regions reveals the lysosome-associated protein Arl8b as a candidate biomarker for Alzheimer's disease. *Genome Med*. 2023;15(1):50.
24. Choi I, Wang M, Yoo S, et al. Autophagy enables microglia to engage amyloid plaques and prevents microglial senescence. *Nat Cell Biol*. 2023;25(7):963—974.
25. Klein WL. Aβ toxicity in Alzheimer's disease: globular oligomers (ADDLs) as new vaccine and drug targets. *Neurochem Int*. 2002;41(5):345—352.
26. Yang N, Zhang K, Guan QW, Wang ZJ, Chen KN, Mao XY. D-penicillamine reveals the amelioration of seizure-induced neuronal injury via inhibiting Aqp11-dependent ferroptosis. *Antioxidants (Basel)*. 2022;11(8):1602.
27. Naeve GS, Vana AM, Eggold JR, et al. Expression profile of the copper homeostasis gene, rAtox1, in the rat brain. *Neuroscience*. 1999;93(3):1179—1187.
28. Zhao P, Shi W, Ye Y, et al. Atox1 protects hippocampal neurons after traumatic brain injury via DJ-1 mediated anti-oxidative stress and mitophagy. *Redox Biol*. 2024;72:103156.
29. Montes S, Rivera-Mancia S, Diaz-Ruiz A, Tristan-Lopez L, Rios C. Copper and copper proteins in Parkinson's disease. *Oxid Med Cell Longev*. 2014;2014:147251.
30. Wu X, Miller JA, Lee BTK, Wang Y, Ruedl C. Reducing microglial lipid load enhances β amyloid phagocytosis in an Alzheimer's disease mouse model. *Sci Adv*. 2025;11(6):eadq6038.
31. Fleiss B, Van Steenwinckel J, Bokobza C, Shearer IK, Ross-Munro E, Gressens P. Microglia-mediated neurodegeneration in perinatal brain injuries. *Biomolecules*. 2021;11(1):99.
32. Cagnin A, Brooks DJ, Kennedy AM, et al. *In-vivo* measurement of activated microglia in dementia. *Lancet*. 2001;358(9280):461—467.
33. Hopperton KE, Mohammad D, Trépanier MO, Giuliano V, Bazinet RP. Markers of microglia in post-mortem brain samples from patients with Alzheimer's disease: a systematic review. *Mol Psychiatry*. 2018;23(2):177—198.
34. Walker DG, Lue LF. Immune phenotypes of microglia in human neurodegenerative disease: challenges to detecting microglial polarization in human brains. *Alzheimers Res Ther*. 2015;7(1):56.
35. Yu CH, Yang N, Bothe J, et al. The metal chaperone Atox1 regulates the activity of the human copper transporter ATP7B by modulating domain dynamics. *J Biol Chem*. 2017;292(44):18169—18177.
36. Kumari N, Kumar A, Pal A, Thapa BR, Modi M, Prasad R. In-silico analysis of novel p.(Gly14Ser) variant of ATOX1 gene: plausible role in modulating ATOX1-ATP7B interaction. *Mol Biol Rep*. 2019;46(3):3307—3313.
37. Yu CH, Lee W, Nokhrin S, Dmitriev OY. The structure of metal binding domain 1 of the copper transporter ATP7B reveals mechanism of a singular Wilson disease mutation. *Sci Rep*. 2018;8(1):581.

38. Banci L, Bertini I, Ciofi-Baffoni S, Kozyreva T, Zovo K, Palumaa P. Affinity gradients drive copper to cellular destinations. *Nature*. 2010;465(7298):645—648.
39. Li F, Cui L, Yu D, et al. Exogenous glutathione improves intracellular glutathione synthesis via the γ-glutamyl cycle in bovine zygotes and cleavage embryos. *J Cell Physiol*. 2019;234 (5):7384—7394.
40. Li W, Meng X, Peng K, et al. Boosting microglial lipid metabolism via TREM2 signaling by biomimetic nanoparticles to attenuate the sevoflurane-induced developmental neurotoxicity. *Adv Sci (Weinh)*. 2024;11(10):e2305989.
41. Heneka MT, Carson MJ, El Khoury J, et al. Neuroinflammation in Alzheimer's disease. *Lancet Neurol*. 2015;14 (4):388—405.
42. Saijo K, Winner B, Carson CT, et al. A Nurr1/CoREST pathway in microglia and astrocytes protects dopaminergic neurons from inflammation-induced death. *Cell*. 2009;137(1):47—59.
43. Drew SC, Barnham KJ. The heterogeneous nature of $Cu^{2+}$Interactions with Alzheimer's amyloid-β peptide. *Acc Chem Res*. 2011;44(11):1146—1155.
44. Adlard PA, Cherny RA, Finkelstein DI, et al. Rapid restoration of cognition in Alzheimer's transgenic mice with 8-hydroxy quinoline analogs is associated with decreased interstitial aβ. *Neuron*. 2008;59(1):43—55.
45. Zheng Z, White C, Lee J, et al. Altered microglial copper homeostasis in a mouse model of Alzheimer's disease. *J Neurochem*. 2010;114(6):1630—1638.
46. Lutsenko S. Human copper homeostasis: a network of interconnected pathways. *Curr Opin Chem Biol*. 2010;14(2): 211—217.
47. Miyayama T, Suzuki KT, Ogra Y. Copper accumulation and compartmentalization in mouse fibroblast lacking metallothionein and copper chaperone, Atox1. *Toxicol Appl Pharmacol*. 2009;237(2):205—213.
48. Kelner GS, Lee M, Clark ME, et al. The copper transport protein Atox1 promotes neuronal survival. *J Biol Chem*. 2000;275(1): 580—584.
49. Muhammad T, Ikram M, Ullah R, Rehman SU, Kim MO. Hesperetin, a *citrus* flavonoid, attenuates LPS-induced neuroinflammation, apoptosis and memory impairments by modulating TLR4/NF-κB signaling. *Nutrients*. 2019;11(3):648.
50. Estaquier J, Vallette F, Vayssiere JL, Mignotte B. The mitochondrial pathways of apoptosis. *Adv Exp Med Biol*. 2012;942: 157—183.
51. Li C, Zhao Z, Luo Y, et al. Macrophage-disguised manganese dioxide nanoparticles for neuroprotection by reducing oxidative stress and modulating inflammatory microenvironment in acute ischemic stroke. *Adv Sci (Weinh)*. 2021;8(20):e2101526.
52. Simpson DSA, Oliver PL. ROS generation in microglia: understanding oxidative stress and inflammation in neurodegenerative disease. *Antioxidants (Basel)*. 2020;9(8):743.
53. Han B, Jiang W, Liu H, et al. Upregulation of neuronal PGC-1α ameliorates cognitive impairment induced by chronic cerebral hypoperfusion. *Theranostics*. 2020;10(6):2832—2848.
54. Gong Y, Tong L, Yang R, et al. Dynamic changes in hippocampal microglia contribute to depressive-like behavior induced by early social isolation. *Neuropharmacology*. 2018;135:223—233.
55. Crews FT, Vetreno RP. Stress and alcohol priming of brain toll-like receptor signaling in alcohol use disorder. *Alcohol Alcohol*. 2018;53(6):639—641.
56. Song XD, Zhang JJ, Wang MR, Liu WB, Gu XB, Lv CJ. Astaxanthin induces mitochondria-mediated apoptosis in rat hepatocellular carcinoma CBRH-7919 cells. *Biol Pharm Bull*. 2011; 34(6):839—844.
57. Yang F, Zhang C, Zhuang Y, et al. Oxidative stress and cell apoptosis in caprine liver induced by molybdenum and cadmium in combination. *Biol Trace Elem Res*. 2016;173(1): 79—86.
58. He L, Zhou G, He Y, et al. Different neurotropic pathogens elicit neurotoxic CCR9- or neurosupportive CXCR3-expressing microglia. *J Immunol*. 2006;177(6):3644—3656.
59. Lei C, Lin S, Zhang C, et al. High-mobility group box1 protein promotes neuroinflammation after intracerebral hemorrhage in rats. *Neuroscience*. 2013;228:190—199.
60. Lu J, Wu DM, Zheng YL, et al. Trace amounts of copper exacerbate beta amyloid-induced neurotoxicity in the cholesterol-fed mice through TNF-mediated inflammatory pathway. *Brain Behav Immun*. 2009;23(2):193—203.